Astronomy
&
Astrophysics

H I observations of giant low surface brightness galaxies[*,**]

L. D. Matthews[1], W. van Driel[2], and D. Monnier-Ragaigne[2,3]

[1] National Radio Astronomy Observatory, 520 Edgemont Road, Charlottesville, VA 22903, USA
[2] Unité Scientifique Nançay, USR CNRS B704, Observatoire de Paris, 5 place Jules Janssen,
92195 Meudon, France
[3] DAEC, UMR CNRS 8631, Observatoire de Paris, 5 place Jules Janssen, 92195 Meudon, France

Abstract. We have used the Nançay Radio Telescope to obtain new global H I data for 16 giant low surface brightness (LSB) galaxies. Our targets have optical luminosities and disk scale lengths at the high end for spiral galaxies ($L_B \sim 10^{10}\ L_\odot$ and $h_r \gtrsim 6$ kpc for $H_0 = 75$ km s^{-1} Mpc^{-1}), but they have diffuse stellar disks, with mean disk surface brightnesses $\gtrsim 1$ magnitude fainter than normal giant spirals. Thirteen of the galaxies previously had been detected in H I by other workers, but the published H I observations were either confused, resolved by the telescope beam, of low signal-to-noise, or showed significant discrepancies between different authors. For the other 3 galaxies, no H I data were previously available. Several of the galaxies were resolved by the Nançay $3'.6$ E-W beam, so global parameters were derived from multiple-point mapping observations. Typical H I masses for our sample are $\gtrsim 10^{10}\ M_\odot$, with $M_{\rm HI}/L_B = 0.3 - 1.7$ (in solar units). All of the observed galaxies have published optical surface photometry, and we have compiled key optical measurements for these objects from the literature. We frequently find significant variations among physical parameters of giant LSB galaxies reported by various workers.

Key words. galaxies: distances and redshifts – galaxies: general – galaxies: ISM – radio lines: galaxies

1. Introduction

1.1. The discovery of giant low surface brightness galaxies

In 1987, Bothun et al. reported the serendipitous discovery of the extraordinarily large low surface brightness (LSB) galaxy now known as Malin-1. In spite of having a projected B-band central surface brightness of only 26.5 mag arcsec^{-2}, Malin-1 is the largest spiral galaxy known, with a disk scale length of 73 kpc (assuming $H_0 = 75$ km s^{-1} Mpc^{-1}), and an exceptionally high H I mass ($\sim 10^{11}\ M_\odot$) and optical luminosity ($M_B = -23.1$). Subsequently, through systematic searches of photographic survey plates, other galaxies with similar (albeit slightly less extreme) properties to Malin-1 have been uncovered (Bothun et al. 1990; Sprayberry et al. 1993; Sprayberry et al. 1995b). We hereafter refer to these

as "LSB Giants". A handful of LSB Giants are also found in the UGC (Nilson 1973), NGC (Dreyer 1953), and ESO (Lauberts & Valentijn 1989) catalogues (see Gallagher & Bushouse 1983; Impey & Bothun 1989; Walsh et al. 1997; Pickering et al. 1997; Schombert 1998). Nonetheless, while recent photographic and CCD surveys have uncovered large numbers of new small and medium-sized, moderate-to-low surface brightness spiral galaxies (e.g., Schombert et al. 1992; Impey et al. 1996; O'Neil et al. 1997), LSB Giants have remained relatively rare. Having faint, diffuse disks, but sizes, H I masses, and luminosities at the high end for disk galaxies, the LSB Giants occupy a unique realm of physical parameters space and may share evolutionary histories distinct from other LSB galaxies (e.g., Hoffman et al. 1992).

Since a continuum of values exists for galaxy properties such as surface brightness, luminosity, and scale length, Sprayberry et al. (1995b) proposed to define LSB Giants as those objects meeting a "diffuseness index" criterion: $\mu_B(0) + 5\log(h_r) > 27.6^1$, where $\mu_B(0)$ is the extrapolated, deprojected B-band disk central surface brightness

---

[*] Tables 2 and 4 are only available in electronic form at the CDS via anonymous ftp to `cdsarc.u-strasbg.fr` (`130.79.128.5`) or via
`http://cdsweb.u-strasbg.fr/cgi-bin/qcat?J/A+A/365/1`
[**] Figure 2 and Tables 3, 5 and 6 are only available in electronic form at `http://www.edpsciences.org`

---

[1] Sprayberry et al. (1995b) formulated their diffuseness index based on a distance scale with $H_0 = 100$ km s^{-1} Mpc^{-1}. Here we have rewritten the diffuseness criterion for $H_0 = 75$ km s^{-1} Mpc^{-1}, which is assumed throughout this work.

in magnitudes arcsec^{-2}, and h_r is the disk scale length in kpc. Among seven LSB Giants described by Sprayberry et al. (1995b), mean properties include: $< B - V >= 0.73 \pm 0.05$, $< \mu_B(0) >= 23.23 \pm 0.19$ mags arcsec^{-2}, and $< h_r >= 13.0$ kpc. The colors of these LSB Giants are thus comparable to those of normal spirals (Sprayberry et al. 1995b), but are redder than typical colors of many small and moderate-sized LSB disks (e.g., McGaugh & Bothun 1994; Matthews & Gallagher 1997; de Blok et al. 1996; Beijersbergen et al. 1999). In addition, the LSB Giants are distinct from other more common LSB spirals in that they often have a significant bulge component (e.g., Gallagher & Bushouse 1983; Knezek 1993, 1998), and frequently their centers harbor an active nucleus (e.g., Schombert 1998).

The origin and evolutionary histories of LSB Giant galaxies are still enigmatic. Hoffman et al. (1992) have proposed a formation scenario whereby these systems form in very low density regions from rare, 3σ density fluctuations. They predict these galaxies should exhibit quiescent, unevolved, gas-rich disks, with rotation curves that flatten near $V_{\max} \sim 300$ km s^{-1}. Knezek (1993) has suggested an alternative scenario, based on Kormendy (1989), whereby LSB Giants may have dissipatively formed from massive, metal-poor dark matter halos.

1.2. The need for new HI observations

Testing formation and evolution scenarios for LSB Giants requires an accurate knowledge of the neutral gas properties and linewidths of these galaxies. And only by combining such measures with optical data can we begin to build a picture of the star-formation histories of these systems and their relationship to other types of LSB galaxies.

Other motivations also exist for improved H I observations. Hoffman et al. (1992) have argued that for the enormous disks of LSB Giants to remain quiescent over a Hubble time, they must be very isolated. Yet studies hint that LSB Giants are in fact less isolated than other LSB spirals, although redshift surveys in the vicinities of these objects are still incomplete (Sprayberry et al. 1995b). Pointed H I observations in the vicinity of LSB Giants can thus reveal if these galaxies have any yet-undiscovered gas-rich neighbors.

Another important use of H I data is for exploring the Tully-Fisher (TF) relation for giant LSB spirals. Sprayberry et al. (1995a) have shown that at least two of the presently known LSB Giant galaxies are extreme outliers from the TF relation defined by normal galaxies. This is unlike the bulk of moderate-sized, moderate luminosity LSB galaxies, which tend to follow TF (Sprayberry et al. 1995a; Zwaan et al. 1995; Verheijen 1997). It is of considerable interest therefore to assess from a larger sample whether LSB Giants deviate systematically from the TF relation.

While previous H I observations have established that LSB Giants are in general very gas-rich ($M_{\mathrm{HI}} \gtrsim 10^{10}\ M_\odot$;

e.g., Sprayberry et al. 1995b; Walsh et al. 1997; Pickering et al. 1997, 1999), unfortunately existing H I data for many LSB Giants are of dubious quality (i.e., the galaxy was confused or resolved by the telescope beam, the spectra are of low signal-to-noise, or measurements from different workers are highly discrepant; see also Table 5 and Sect. 4).

For example, based on Arecibo 21-cm observations of 3 objects, Sprayberry et al. (1995b) suggested that peculiar, asymmetric H I profiles may be commonplace for LSB Giants. However, since the H I extents of these galaxies were expected to be comparable to the size of the telescope beam, it is important to verify that these "peculiar" spectra do not result from some combination of source resolution and telescope mispointing. In addition, independent checks on derived H I parameters are valuable since it is more difficult to accurately measure integrated fluxes and linewidths when the global H I profiles are quite broad compared to the bandwidth used, and when sources are at large recessional velocities ($V_r \gtrsim 15\,000$ km s^{-1}), where flux calibration can become increasingly uncertain. Finally, there are still a handful of known LSB Giants for which no H I data have previously been obtained.

Quality single-dish H I spectra for LSB Giants are also a useful precursor and complement to H I aperture synthesis studies of these galaxies (e.g., Walsh et al. 1997; Pickering et al. 1997, 1999). H I mapping is of course a critical part of understanding the dynamics and gas distributions for these galaxies, but since many of the known examples of LSB Giants are rather distant ($V_r > 10\,000$ km s^{-1}) and of relatively modest optical angular size ($D_{25} < 2'$), such observations are challenging and benefit from careful planning based on prior H I measurements. Moreover, because LSB Giants are generally expected to have disks with relatively low H I surface densities (e.g., Pickering et al. 1997), diffuse emission can be missed in aperture synthesis measurements, and total flux and maximum rotational velocity measures from H I pencil beam observations serve as an important check.

Based on the above motivations, we have used the Nançay Radio Telescope to obtain new global observations of a sample of 16 LSB Giant galaxies for which existing global H I measurements were incomplete, required reconfirmation, or were nonexistent. We measure integrated H I line fluxes, linewidths, and recessional velocities, and attempt to clear up conundrums surrounding several of these objects in the literature.

2. Sample selection

Our targets for the present program were 16 LSB Giant galaxies meeting the "diffuseness" criterion stated in Sect. 1. The objects were culled from Knezek (1993), Sprayberry et al. (1995b), and Pickering et al. (1997), and all have available optical surface photometry. Thirteen of our targets have previously been observed in H I by other workers, but the published H I parameters were uncertain or incomplete (see below). For the other 3 galaxies,

Table 1. Basic parameters for target galaxies compiled from NED and LEDA

Ident.	RA	Dec	Classification		$m_{\rm b}$	D_{25}	b/a	i	PA	$V_{\rm r}$	$\sigma(V)$
	(1950.0)		LEDA	NED	mag	$'$		$^\circ$	$^\circ$	km s^{-1}	km s^{-1}
UGC 568	00 52 35.5	−01 19 01	S?	Sd	15.08	1.17	0.70	40		13197	204
UGC 1752	02 13 30.0	24 40 00	Sc	SA(s)cd	16.5	1.55	1.00	0:	0:	17847	60
PGC 135657	02 37 38.7	−01 59 18	Sb	Sc	15.47	0.78		38	63	12701	60
UGC 2936	04 00 12.6	01 49 36	SBc	SB(s)d	15.00	2.51	0.27	78	30	3817	125
UGC 3140	04 40 20.1	00 31 35	Sbc	SA(rs)c:	13.30	1.78	0.91	0:	175	4633	60
NGC 2770	09 06 29.8	33 19 53	Sc	SA(s)c:	12.77	3.66	0.30	79	148	1947	63
PGC 135754	10 34 52.9	02 20 57	Sc	Sc	16.34			49		21335	60
F568-6	10 37 08.5	21 06 24	Scd	Sd/p	15.28	1.67	0.79	38		13830	
UGC 6614	11 36 39.1	17 25 14	Sa	(R)SA(r)a:	14.37	2.02	0.86	35	0:	6351	60
Malin-1	12 34 27.3	14 36 15		S	16.20	0.20	0.93	45	45	24750	
PGC 45080	13 00 42.6	01 44 12	Sc	Sc	15.61	0.79	0.22	72	84	12264	295
UGC 9024	14 04 21.0	22 18 28	Sa	S:	16.0	2.09	0.95	37	0:	2323	
F530-1	21 05 21.5	26 15 00	Sc	S(r)	16.31	0.47	0.74			14340	
F533-3	22 14 53.3	24 57 48	SBc	SBc(r)	15.43	0.88	0.65	65:	165:	12669	
NGC 7589	23 15 41.9	−00 00 45	Sb	SAB(rs)a:	15.01	1.07	0.62	58	60	8938	219
PGC 71626	23 27 58.2	−02 44 18	SBc	SB(r)b pec	15.14	1.78	0.59	61	65	9520	247

no H I data were previously available. Some basic parameters for our target galaxies are summarized in Table 1. Coordinates, B magnitudes, angular sizes, axial ratios, and radial velocities were culled from the NED database. Position angles and scatter in the published radial velocity values [$\sigma(V)$] were taken from the LEDA database, and inclinations were obtained from the various references given in Table 6 (discussed below). Inclinations and position angles marked with a colon (:) were estimated by us from inspection of the Digitized Sky Survey.

3. Observations

3.1. Data acquisition

The Nançay decimentric radio telescope is a meridian transit-type instrument of the Kraus/Ohio State design, consisting of a fixed spherical mirror (300 m long and 35 m high), a tiltable flat mirror (200 × 40 m), and a focal carriage moving along a curved rail track. Due to an ongoing major renovation of the focal system, the length of the focal track was reduced to ∼60 m during the period of our observations, thus allowing tracking of a source on the celestial equator for about 45 min. The effective collecting area of the Nançay telescope is roughly 7000 m^2 (equivalent to a 94-m diameter parabolic dish). Due to the elongated geometry of the mirrors, at 21-cm wavelength the Nançay telescope has a half-power beam width of 3.6 E-W × 22′ N-S for the range of declinations covered in this work (E. Gérard, private comm.; see also Matthews & van Driel 2000). Typical system temperatures were ∼40 K for our project.

The observations at Nançay were made in the period June 1998 - October 1999, using a total of about 300 hours of telescope time. We obtained our observations in total power (position-switching) mode using consecutive pairs of two-minute on- and two-minute off-source integrations. Off-source integrations were taken at approximately 20′ E of the target position. The autocorrelator was divided into two pairs of cross-polarized receiver banks, each with 512 channels and a 6.4 MHz bandpass. This yielded a channel spacing of 2.64 km s^{-1}, for an effective velocity resolution of ∼3.3 km s^{-1} at 21-cm. The center frequencies of the two banks were tuned to the expected redshifted H I frequency of the target based on values from the literature (Table 1). Depending on the signal strength, the spectra were smoothed to a channel separation of ∼7.9 or ∼13.2 km s^{-1} during the data reduction in order to increase signal-to-noise. Total integration times were up to 12 hours per galaxy, depending on the strength of the source and scheduling constraints.

In all cases, data were initially obtained with the telescope pointed at the published optical center of the galaxy. However, as shown by van der Hulst et al. (1993), the H I disks of large LSB spirals may frequently extend to up to ∼2.5× their optical diameter. We therefore observed several of the targets, including the 8 galaxies with $D_{25} \gtrsim 1.3$ (i.e. one-third the Nançay FWHP E-W beamwidth) at three or more spatial positions: one at the target's optical center, plus additional pointings offset to the east or west by multiples of one-half beamwidth (see Table 3, discussed below). Because of the large N-S diameter of the Nançay beam (≥22′), these mapping observations were limited to pointings along an E-W line.

3.2. Calibration

Flux calibration (i.e., $T_{\rm sys}$-to-mJy conversion) at Nançay is determined via regular measurements of a cold load calibrator and periodic monitoring of strong continuum sources by the Nancay staff. Standard calibration procedures include correction for declination-dependent gain

variations of the telescope (e.g., Fouqué et al. 1990). These techniques typically yield an internal calibration accuracy of ~15% at frequencies near 1420 MHz.

In our present program several of our targets have recessional velocities $V_r \geq 12\,000$ km s^{-1} and hence were observed at frequencies where calibration reliability and consistency at Nançay and other radio telescopes are less well established. To estimate the comparative accuracy of our flux density calibration at these lower frequencies as well as recheck frequency dependent changes in the noise diode temperature, we examined continuum calibration data obtained at 1400, 1425, and 1280 MHz, from several periods over the course of the months during which our spectral line data were acquired (L. Alsac, private comm.; see also Thuan et al. 2000). Over this frequency range we found the noise diode temperature to vary by less than 10%. Our data were corrected for this effect based on a linear correction curve derived from the continuum data. These calibration data also confirm the expected internal calibration accuracy of our data is $\sim \pm 15\%$ near 1420–1425 MHz, but only $\sim \pm 25\%$ near 1280 MHz.

An additional step was required for accurate flux calibration of our Nançay data, as it has been found that changes have occurred in the output power of the calibration diode used at Nançay since the early 1990's (see Fig. 4 of Theureau et al. 1998; see also Thuan et al. 2000), resulting in an overall shift of the absolute calibration scale. This makes it necessary to appropriately renormalize the fluxes determined via the standard calibration techniques described above (e.g., Theureau et al. 1998; Matthews et al. 1998; Thuan et al. 2000).

Matthews et al. (1998) showed via a statistical comparison of integrated fluxes measured for ~30 galaxies at Nançay and elsewhere that applying a scaling factor of 1.26 to the Nançay flux densities very effectively corrects for the above effect, and restores the correct normalization of the Nançay flux scale. Matthews & van Driel (2000) subsequently found that the application of this same factor minimized scatter between fluxes determined for a second sample of galaxies observed at both Nançay and at Arecibo. Theureau et al. (1998 and priv. comm.) also derived similar corrections via independent observations of line calibration sources. As a final calibration step we therefore apply a renormalization factor of 1.26 to all fluxes reported in the present work.

3.3. Data reduction

We reduced our H I spectra using the standard DAC and SIR Nançay spectral line reduction packages available at the Nançay site. With this software we subtracted baselines (generally third order polynomials), averaged the two receiver polarizations, and applied a declination-dependent conversion factor to convert from units of T_{sys} to flux density in mJy. Because of the broad width of the lines, careful attention was paid to baseline fitting, and scans with extremely curved baselines were discarded.

In addition, the reductions were performed independently by two of us to check the consistency of the results.

3.4. Measurement of HI parameters from global spectra

Radial velocities, V_{HI}, peak flux densities, integrated line fluxes, velocity widths at 50% and 20% of peak maximum (W_{50} and W_{20}), and rms noise levels of our program spectra were measured using our own IDL software. Velocity widths were measured interactively, by moving the cursor outward from the profile center. Radial velocities were defined to be the centroid of the two 20% peak maximum points on the profile and are quoted using the optical convention.

3.5. Analysis of mapped galaxies

To construct the global H I profiles for each of the mapped galaxies, we employed the procedure of Matthews et al. (1998). A Gaussian model with appropriate sidelobes for the Nançay beam was assumed (see Guibert 1973). We treated the beam as infinite in the N-S direction, thus reducing the analysis to a one-dimensional problem. With our model beam, the model galaxy flux distributions were then iteratively integrated numerically until the best-fit model that reproduced the observed flux distribution in each of the telescope pointings was found.

In all cases an asymmetric Gaussian H I distribution (i.e., a lopsided Gaussian with a different σ on the E and W sides, but uniform height) was assumed for the H I distribution of the galaxy. Because all of our sample galaxies were only coarsely resolved by the Nançay beam in the E-W direction, use of models for the H I distribution more complex than a Gaussian (e.g., containing central H I depressions, etc.) was not attempted (see also Fouqué 1984). Moreover, we found the simple Gaussian models produced a good match to the data in all but two cases (F568-6 & F533-3; see Sect. 4).

3.6. Global HI spectra and measured HI parameters

Our reduced Nançay global H I spectra for all of our target galaxies are shown in Fig. 1. For the mapped galaxies, the spectra at each individual pointing are shown in Fig. 2.

Parameters for the final global spectra for all of our targets, including the mapped galaxies, are given in Table 2. The columns in Table 2 are defined as follows:
(1) Galaxy name;
(2) Spectrum rms, in millijanskys;
(3) Peak flux density of the line profile, in millijanskys;
(4) & (5) Raw, measured full width at 20% and 50% of the maximum profile height, respectively, in km s^{-1}. No correction has been applied to the raw linewidths for cosmological stretching, instrumental resolution, or for the errors arising from describing equal frequency-width channels by a constant velocity width across the entire bandwidth
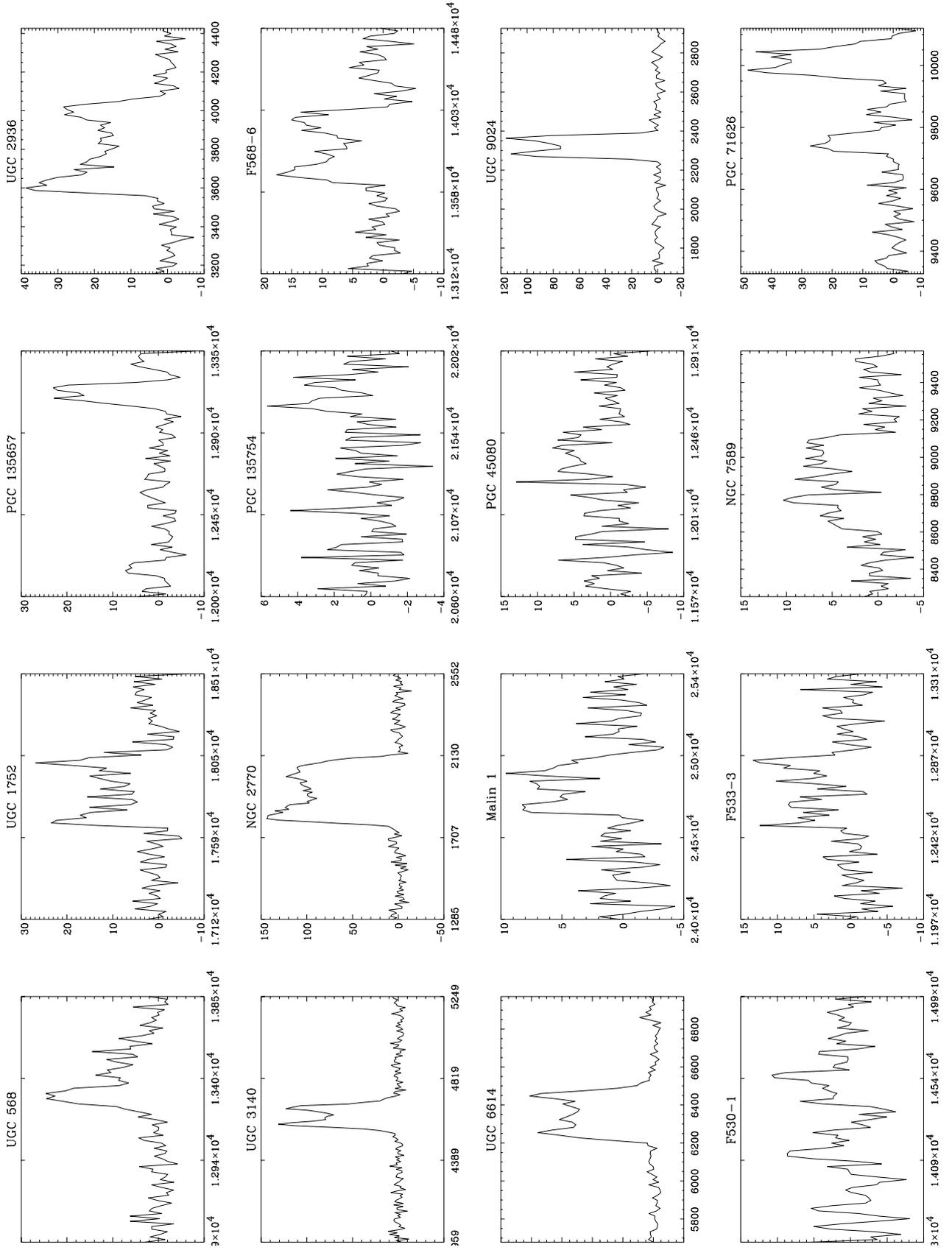
Fig. 1. Nançay global H I 21-cm line spectra of 16 Giant low surface brightness galaxies. Axes are flux density, in millijanskys, and radial velocity, in km s^{-1}, using the optical convention. The spectra shown have been smoothed to velocity resolutions of $\sim$8 or 13 km s^{-1}

of the spectrum (but see Table 4). The latter effect is inherent in the Nançay software, but is negligible $\lesssim 1.5$ km s^{-1}) compared with our measurement uncertainties;

(6) Heliocentric radial velocity, in km s^{-1}, quoted using the optical convention, $V_{\mathrm{HI}} = c(\nu_0 - \nu)/\nu$;

(7) Uncertainty in the heliocentric radial velocity, in km s^{-1} computed following the prescription of Fouqué et al. (1990). Errors in the measured linewidths may be estimated as $\sigma(W_{20}) \approx 3\sigma(V)$ and $\sigma(W_{50}) \approx 2\sigma(V)$ (Fouqué et al. 1990);

(8) Raw, integrated H I line flux, in Jy km s^{-1}. No corrections have been applied for beam attenuation;

(9) Uncertainty in the integrated line flux, in Jy km s^{-1}, computed following Fouqué et al. (1990);

(10) Signal-to-noise ratio of the detected line, defined as the ratio of the peak flux density to the spectrum rms;

(11) Comments. For more detailed comments on individual spectra, see Sect. 4.

Table 3 summarizes the raw, integrated line profile fluxes (S_{HI}) and velocity centroids (V_c) for each pointing in our mapping observations. In cases where no flux was detected at a particular pointing, a 1σ upper limit to the integrated flux was estimated simply by multiplying the rms noise of the spectrum by the linewidth at 50% peak maximum from the previous pointing.

In Table 4 we tabulate several additional parameters for our target galaxies. Columns in Table 4 are as follows:
(1) Galaxy name;

(2) & (3) W_{20} and W_{50} values corrected for cosmological stretching and spectral resolution, using the relation

$$W_{\mathrm{w,cor}} = [W_{\mathrm{w,raw}} + \delta_c]/(1+z) \qquad (1)$$

(see Haynes & Giovanelli 1984). Here $W_{\mathrm{w,raw}}$ is the raw observed linewidth at $w = 20\%$ or $w = 50\%$ peak maximum, $z = V_{\mathrm{HI}}/c$, and δ_c is given by

$$\delta_c = (0.014\omega - 0.83)\delta_{\mathrm{R}} \qquad (2)$$

where $\omega = 20$ and $\omega = 50$ for W_{20} and W_{50}, respectively, and δ_{R} is the velocity resolution of the measured spectrum (see Bottinelli et al. 1990). No corrections were applied for inclination angle of the source or for turbulent motions;

(4) Radial velocity, in km s^{-1}, corrected to the Local Standard of Rest, following the prescription of Sandage & Tammann (1981):

$$V_{\mathrm{LSR}} = V_{\mathrm{HI}} - 79\cos l\cos b + 296\sin l\cos b$$
$$- 36\sin b \ \mathrm{km\,s^{-1}}; \qquad (3)$$

(5) Galaxy distance in Mpc, computed from $D = V_{\mathrm{LSR}}/H_0$;

(6) Logarithm of the H I mass in solar units, computed from the integrated line flux S_{HI} in Col. 8 of Table 2 and using the relation $M_{\mathrm{HI}} = 2.36 \ 10^5 D^2 S_{\mathrm{HI}}$;

(7) Ratio of the M_{HI} mass to the optical B-band luminosity L_B, in solar units. L_B was derived from the mean of the absolute B magnitudes for each galaxy given in Table 6 (discussed below) and assuming a solar absolute magnitude of $M_{B,\odot} = 5.48$. For NGC 7589 a B-band magnitude was taken from the NED database;

(8) Rough estimate of the H I diameter of the source in arcminutes. Estimates were made only for mapped galaxies where flux was detected at 2 or more positions (see Table 3). Following Fouqué (1984), we define the H I diameter as the isophote enclosing half of the H I mass in a flat H I disk model, which for a Gaussian H I surface density, is equal to the FWHM of the model (Fouqué 1984). Because of the elongation of the Nançay beam and the fact that our maps were obtained along an E-W axis, a correction to the raw H I diameter for the position angle and inclination of the source was also applied. Hence,

$$D_{\mathrm{HI}} = Q^{-1}D_{\mathrm{HI}}^{\mathrm{EW}} \qquad (4)$$

where:

$$Q^2 = \sin^2(\mathrm{PA}) + R_{\mathrm{H}}^{-2}\cos^2(\mathrm{PA}). \qquad (5)$$

Here, R_{H} is the ratio of the major to the minor axis of the H I distribution and PA is the position angle of the major axis. We assume $R_{\mathrm{H}} = (a/b)_{\mathrm{optical}}$ and adopt the photometric position angle for PA (Fouqué 1984). Typical errors for this method of estimating D_{HI} are $\sim 30 \pm 30\%$ (see Fouqué 1984).

4. Discussion

4.1. The HI properties of LSB Giants

Not surprisingly, all of the LSB Giant galaxies observed in the present program are found to be very H I-rich systems, having M_{HI} values ranging from 2.5 10^9 $M_{\odot}$– 7.1 10^{10} $M_{\odot}$(Table 4). The bulk of the sample galaxies are not only H I rich in an absolute sense, but are also H I-rich both for their Hubble types and for their optical luminosities – six of the galaxies in the present LSB Giant sample have $M_{\mathrm{HI}}/L_B \gtrsim 1$ (in solar units; see Table 4). More typical values of M_{HI}/L_B for high surface brightness spirals are: ~ 0.2 (type Sab-Sb); ~ 0.3 (type Sbc-Sc); ~ 0.4 (type Scd-Sd) (Roberts & Haynes 1994).

As expected for massive, H I-rich disks, broad H I linewidths are also hallmarks of LSB Giants. Because a number of our program galaxies have rather low inclinations ($i \leq 40°$), it is difficult to estimate the true rotational velocities in some cases, but even many of the uncorrected linewidths tend to be quite broad (e.g., $W_{20,c} = 398$ km s^{-1} for UGC 1752, which is seen nearly face-on). Only PGC 71626 seems to have a surprisingly narrow linewidth ($W_{20,c} = 115$ km s^{-1}) given its inclination ($i = 61°$) and Hubble type (SBb or SBc).

The majority of the LSB Giants in our study exhibit relatively normal, classic, double-horned rotational profiles (Fig. 1). However, we do see a few unusual cases as well; UGC 568 shows a peculiar, strongly asymmetric profile; PGC 45080 and NGC 7589 both have rather squarish

global profiles with no clear rotation horns; and finally, F530-1 has a double-horned profile that is strongly "cleft" in the middle. PGC 135754 may also have a similar cleft morphology, but our detection of this source is relatively weak. Among the 11 relatively normal, double-horned profiles, 3 cases show modest asymmetries (UGC 2936, NGC 2770, and F568-6). Thus we find no evidence that strong H I asymmetries are a general feature of LSB Giants. We comment further on our individual spectra below.

4.2. Comparison of new HI data with previous measurements and comments on individual objects

In order to compare the H I parameters derived in the present work with past measurements, we have compiled global H I parameters from the literature for the 13 of our sample galaxies which have previously been observed in the 21-cm line. Table 5 summarizes previously measured recessional velocities, linewidths, and integrated line fluxes for each case, and indicates the telescope at which the data were obtained, as well as the reference for the quoted parameters.

An examination of Table 5 shows that for LSB Giants observed by more than one group, significant discrepancies frequently exist between the measured parameters, particularly the global integrated line fluxes. We discuss each of the 16 targets observed in the present work in more detail below, including comments on these discrepancies. As part of our investigation of our LSB Giant targets, we also searched the vicinity of each of the 16 objects (i.e., an area about 1.5 times the Nançay HPBW) for nearby galaxies which could possibly give rise to confusion in our observed H I profiles. For this we employed the NED and LEDA databases, as well as optical images extracted from the Digitized Sky Survey (DSS). Results of these searches are also described below.

UGC 568: No H I data have been previously published for this object. Our global spectrum appears quite peculiar, having a strong asymmetry, with a broad, single "horn" on the low velocity side of the profile. Published optical redshifts show a discrepancy of over 400 $\mathrm{km\,s^{-1}}$ ($V_{\mathrm{opt}} = 13\,600$ $\mathrm{km\,s^{-1}}$, Melnick & Quintana 1981; $V_{\mathrm{opt}} = 13\,198 \pm 275$ $\mathrm{km\,s^{-1}}$, Impey et al. 1996). Our new H I velocity corresponds to the mean of the optical redshifts. Several other galaxies were found within our search area, but they do not seem candidates for an H I confusion that could explain our peculiar global H I profile: CGCG 384-029 is a $B_{\mathrm{T}} = 15.0$ mag Sbc spiral with an optical velocity 886 $\mathrm{km\,s^{-1}}$ higher than the LSB Giant (Dale et al. 1998; Katgert et al. 1998), while PGC 3280 is an S0 with a recessional velocity 1524 $\mathrm{km\,s^{-1}}$ lower than the LSB; MCGG +00-03-027 is a 15.5 mag galaxy without known velocity, but it is classified as S0/a (LEDA) or Sa (NED), and is therefore expected to be gas-poor.

UGC 1752: Our new total integrated H I flux ($S_{\mathrm{HI}} = 5.13$ $\mathrm{Jy\,km\,s^{-1}}$) is somewhat larger than that measured at Arecibo by Giovanelli & Haynes (1989; $S_{\mathrm{HI}} = 3.93$ $\mathrm{Jy\,km\,s^{-1}}$), suggesting this galaxy has extended H I emission.

PGC 135657: No H I data have been previously published for this object. Our H I detection has a recessional velocity 407 $\mathrm{km\,s^{-1}}$ larger than the optical velocity of $V_{\mathrm{opt}} = 12\,701 \pm 275$ $\mathrm{km\,s^{-1}}$ reported for PGC 135657 by Impey et al. (1996). In the present survey we detect additional marginal features at the edges of our bandpass, near $V_{\mathrm{HI}} = 12\,100$ $\mathrm{km\,s^{-1}}$ and $V_{\mathrm{HI}} = 13\,300$ $\mathrm{km\,s^{-1}}$. There are a number of small angular size galaxies in this field, but none appear as obvious candidates for interlopers.

UGC 2936: The Arecibo spectrum of UGC 2936 published by Sprayberry (1995b) is highly asymmetric; however only a modest asymmetry is seen in our new data and in the VLA spectrum of Pickering et al. (1999). Our new integrated line flux of 11.23 $\mathrm{Jy\,km\,s^{-1}}$ agrees to within errors with that of Tifft & Cocke (1988) (~ 11.7 $\mathrm{Jy\,km\,s^{-1}}$). In comparison, the Arecibo spectra by Hewitt et al. (1983), Haynes & Giovanelli (1984), and Sprayberry et al. (1995b) all yield considerable lower integrated line fluxes (~ 8.4–9.0 $\mathrm{Jy\,km\,s^{-1}}$), while our new integrated flux value is somewhat lower than the Arecibo measurement of Haynes et al. (1999; 13.29 $\mathrm{Jy\,km\,s^{-1}}$) and the VLA measurement of Pickering et al. (1999; 13.6 $\mathrm{Jy\,km\,s^{-1}}$).

CO(1–0) and CO(2–1) line emission were detected from UGC 2936 at SEST and IRAM by Chini et al. (1996), making this one of the rare galaxies classified as an LSB Giant that has been detected in CO (see also Knezek 1993, 1998). However, Schmelz et al. (1986) failed to detect OH line absorption from the object.

UGC 3140 (= NGC 1642): This galaxy forms a wide pair (8.3 projected separation; $\Delta V_{\mathrm{opt}} = 332 \pm 85$ $\mathrm{km\,s^{-1}}$) with 15.0 mag Sb spiral UGC 3141. Their E-W separation is 3.3 and our Nançay spectrum does not appear to be confused. Our new linewidth measurements are in good agreement with the Jodrell Bank measurements of Staveley-Smith & Davies (1988) and measurements we performed from new HIPASS data (see Barnes et al., in prep. for a description of HIPASS), but are lower than the values published by Bottinelli et al. (1982). No published H I observations are available for UGC 3141.

NGC 2770: Short Westerbork radio synthesis 21-cm line observations (Rhee & van Albada 1996; Broeils & Rhee 1997) indicate that the H I distribution of NGC 2770 at a surface density level of 1 $M_{\odot}$ $\mathrm{pc^{-2}}$ is about 1.7 times as large as the optical (D_{25}) diameter and that its mean H I surface density averaged over the entire H I disk $<\sigma_{\mathrm{HI}}>$ is 4.5 $M_{\odot}$ $\mathrm{pc^{-2}}$, which is higher than typical values for an Sc. Our new spectra show a slightly higher peak flux density on the low-velocity side of the global line profile, hinting at a possible weak asymmetry not seen in the Westerbork observations.

PGC 135754: No H I data have been previously published for this object and it was only weakly detected

in the present study. Our new H I velocity is 434 $km\,s^{-1}$ higher than the optical value reported by Impey et al. (1996; 21335 ± 275 $km\,s^{-1}$).

F568-6 (= Malin-2 = PGC 86622): H I flux appears to have been missed in the Arecibo observations of F568-6 by Schombert et al. (1992). Our new value of $S_{HI} = 4.20$ $Jy\,km\,s^{-1}$ shows good agreement with the value derived from the VLA observations of Pickering et al. (1997; 4.4 $Jy\,km\,s^{-1}$).

UGC 6614: Our new integrated H I flux of 15.94 $Jy\,km\,s^{-1}$ is significantly larger than previous measurements from Arecibo (Bothun et al. 1985a; Haynes & Giovanelli 1989). However, Pickering et al. (1997) measured $S_{HI} = 15.0$ $Jy\,km\,s^{-1}$ from VLA data, consistent with our results. Our H I diameter estimate for this object is very poorly constrained, as we find a Gaussian H I model gives a poor fit to the data. This is reaffirmed by the VLA data of Pickering et al. (1997), which show a significant central depression in the H I distribution of this galaxy.

Malin-1 (= PGC 42102): One published Arecibo observation of Malin-1 (see Table 5) gives an integrated H I line flux (2.5 $Jy\,km\,s^{-1}$; Bothun et al. 1987) comparable to the VLA value derived by Pickering et al. (1997), while a re-reduction of the same Arecibo data yielded $S_{HI} = 3.5$ $Jy\,km\,s^{-1}$ (Impey & Bothun 1989); finally Impey & Bothun (1989) measure $S_{HI} = 4.6$ $Jy\,km\,s^{-1}$ from a Green Bank 43 m spectrum. Our new data indicate that the Arecibo and Green Bank fluxes previously reported by Impey & Bothun (1989) are likely to be significantly overestimated. In contrast our new integrated flux (1.80 $Jy\,km\,s^{-1}$) is somewhat lower than the VLA measurement of Pickering et al. (1997), although our values marginally agree to within errors, since at the redshifted frequency of Malin-1 ($\sim$ 1312 MHz), our absolute calibration uncertainties are expected to be as high as $\sim \pm25\%$ (see Sect. 3.2). In terms of spectral morphology, our new global spectrum shows excellent agreement with that derived by Pickering et al.

No CO(1–0) line emission was detected in the central regions of Malin-1 by Radford (1992), with an estimated upper limit of $4.7\,10^9$ $M_\odot$ to the H_2 mass, and Braine et al. (2000) recently reported an upper limit of $M_{H2}/M_{HI} < 0.03$.

PGC 45080: Our new integrated line flux is smaller than the values reported by Sprayberry et al. (1995b), and our new spectrum lacks the distinct rotation horns seen in the Sprayberry et al. data. Given the small optical size of this object ($D_{25} = 0.'79$) it seems unlikely significant flux extended outside our beam. There are also no obvious interlopers in this field that would have caused confusion in the Sprayberry et al. spectrum, hence the discrepencies in the two spectra are probably due to the lower signal-to-noise of our present data.

UGC 9024: Our new integrated flux value of 11.41 $Jy\,km\,s^{-1}$ is higher than past values measured at Arecibo or with single-pointing Nançay measurements (Bothun et al. 1985; Lewis 1987; Haynes et al. 1997; Theureau et al. 1998), suggesting this galaxy has extended H I emission.

F530-1 (= PGC 87136): We detect only a slightly higher integrated flux (2.07 $Jy\,km\,s^{-1}$) than the Arecibo value of Schombert et al. (1992; 1.7 $Jy\,km\,s^{-1}$). Our spectrum shows an unusual "cleft" morphology, although our signal-to-noise is only modest due to the broad linewidth of this source.

F533-3 (= PGC 68495): No flux is clearly detected at 2'E in our mapping observations of this galaxy; this may be due to the broadness and relative weakness of the line profile and/or an H I distribution that is very lopsided relative to the optical center of the galaxy. As a result, our H I diameter estimate for F533-3 very uncertain.

NGC 7589: NGC 7589 was mapped in H I at the VLA by Pickering et al. (1997). Our new H I profile hints at a possible small amount of additional flux on the low-velocity side of the profile compared with the VLA global spectrum; this is probably caused by confusion with F893-29, which was also detected in H I at the VLA. F893-29 is a 17.1 mag Sb? spiral (NED) or dwarf (Pickering et al. 1997), 3.'3 SW of the LSB Giant, with a E-W separation of 2.'2. F893-29 has a systemic H I velocity of 8768 $km\,s^{-1}$ (Pickering et al. 1997), consistent with the velocity of the "extra" flux we observe associated with our global profile of NGC 7589. Our new integrated line flux (2.96 $Jy\,km\,s^{-1}$) agrees well with that reported by Pickering et al (1997; 2.7 $Jy\,km\,s^{-1}$), hence the flux contamination from this second source appears to be minimal. However our line profile widths appear to be overestimated by $\sim$100 $km\,s^{-1}$ due to this second source, hence corrections have been applied to the W_{20} and W_{50} measurements in Tables 2 and 4.

PGC 71626: PGC 71626 was detected at a recessional velocity consistent with that recently reported by Theureau et al. (1998), but somewhat offset from the published optical velocity of 9520 $km\,s^{-1}$ reported by Sprayberry et al. (1995b) and Impey et al. (1996). Our new integrated flux value of 3.94 $Jy\,km\,s^{-1}$ is higher than the value of 2.6 $Jy\,km\,s^{-1}$ reported by Theureau et al. (1998) based on a single-pointing Nançay observation. An additional H I source was detected in our spectrum at $V_{HI} = 9753 \pm 4$ $km\,s^{-1}$, with $W_{20} = 73$ $km\,s^{-1}$ and $S_{HI} = 1.52 \pm 0.48$ $Jy\,km\,s^{-1}$. This may be contamination from the S? galaxy MCG -01-59-026 (of unknown redshift), at a projected distance of 4.'5 from PGC 71626, or due to an uncatalogued LSB dwarf visible on the DSS.

4.2.1. Optical parameters for the LSB Giants

All of the LSB Giant galaxies observed in the present survey have optical surface photometry available in the literature. To offer a more complete picture of the nature of the objects in our sample, we have compiled a summary of several optical and photometric parameters for each galaxy in Table 6.

Radial velocities quoted in Table 6 are heliocentric values derived from optical measurements. $B_{\rm tot}$ values are the total B-band magnitudes derived from extrapolated exponential disk fits unless otherwise noted. $\mu(0)$ is the extrapolated central disk surface brightness in the B-band (unless otherwise specified) and is *uncorrected* for inclination and internal extinction. $h_{\rm r}$ is the exponential disk scale length in kpc. M is the absolute magnitude (B-band, unless otherwise noted) derived from the total magnitude in Col. 3, and assuming $D = V_{\rm opt}/H_0$ if no distance was given in the original reference; no internal extinction corrections were applied. Corrections to the values in Table 6 for Galactic extinction, k-corrections, and cosmological surface brightness dimming were generally applied by the original authors.

The values given in Table 6 show that there is a great deal of scatter in the photometric parameters reported for LSB Giant galaxies. Surface photometry of LSB galaxies is always challenging, but it is further complicated for LSB Giants by the fact that many of these galaxies have significant bulges, leading to ambiguity in the bulge-disk decompositions and hence vastly different derived scale lengths and central surface brightness values from different workers. Offsets between recessional velocities derived via optical and H I observations are also common (cf. Table 5).

We include Table 6 partly as a caution to readers interested in understanding the global properties of Giant LSB galaxies that there still exist large uncertainties in the measured parameters for such objects, and to highlight the need for additional surface photometry (and H I measurements) of such galaxies. Such data will be necessary before we can distinguish whether all LSB Giants such as the ones in the present study form a distinct class of object, as suggested by Hoffman et al. (1992), or whether some or most of these objects may form a natural and continuous extension of other low and moderate surface brightness disk galaxies. Well-established photometric parameters will also be key to placing the LSB Giant galaxies on the Tully-Fisher diagram.

References

Beijersbergen, M., de Blok, W. J. G., & van der Hulst, J. M. 1999, A&A, 351, 903

Bothun, G. D., Aaronson, M., Schommer, R. A., et al. 1985a, ApJS, 57, 423

Bothun, G. D., Beers, T. C., & Mould, J. R. 1985b, AJ, 90, 2487

Bothun, G. D., Impey, C. D., Malin, D. F., & Mould, J. R. 1987, AJ, 94, 23

Bothun, G. D., Schombert, J. M., Impey, C. D., & Schneider, S. E. 1990, ApJ, 360, 427

Bottinelli, L., Gouguenheim, L., Fouqué, P., & Paturel, G. 1990, A&AS, 82, 391

Bottinelli, L., Gouguenheim, L., & Paturel, G. 1982, A&A, 113, 61

Braine, J., Herpin, F., & Radford, S. J. E. 2000, A&A, 358, 494

Broeils, A. H., & Rhee, M.-H. 1997, A&A, 324, 877

Chengalur, J. N., Salpeter, E. E., & Terzian, Y. 1993, ApJ, 419, 30

Chini, R., Krügel, E., Lemke, R. 1996, A&AS, 118, 4

Dale, D. A., Giovanelli, R., Haynes, M. P., et al. 1998, AJ, 115, 418

de Blok, W. J. G., McGaugh, S. S., & van der Hulst, J. M. 1996, MNRAS, 283, 18

de Jong, R. S. 1996, A&AS, 118, 557

Dreyer, J. L. E. 1953, A New General Catalogue of Nebulae and Clusters of Stars, London Royal Astronomy Society

Fisher, J. R., & Tully, R. B. 1981, ApJS, 47, 139

Fouqué, P. 1984, A&AS, 55, 55

Fouqué, P., Bottinelli L., Durand, N., Gouenheim, L., & Paturel, G. 1990, A&AS, 86, 473

Gallagher, J. S., & Bushouse, H. 1983, AJ, 88, 55

Giovanelli, R., & Haynes, M. P. 1989, AJ, 97, 633

Guibert, J. 1973, A&AS, 12, 263

Haynes, M. P., & Giovanelli, R. 1984, AJ, 89, 758

Haynes, M. P., Giovanelli, R., Herter, T., et al. 1997, AJ, 113, 1197

Haynes, M. P., Giovanelli, R., Chamaraux, P., et al. 1999, AJ, 117, 2039

Hewitt, J. N., Haynes, M. P., & Giovanelli, R. 1983, AJ, 88, 272

Hoffman, Y., Silk J., & Wyse, R. F. G. 1992, ApJ, 388, L13

Huchra, J., Davis, M., Tonry, J., & Latham, D. 1983, ApJS, 52, 89

Huchtmeier, W. K., & Richter, O.-G. 1989, A General Catalogue of H I Observations of Galaxies (Springer-Verlag)

Impey, C., & Bothun, G. 1989, ApJ, 341, 89

Impey, C. D., Sprayberry, D., Irwin, J. A., & Bothun, G. D. 1996, ApJS, 105, 209

Katgert, P., Mazure, A., den Hartog, R., Adami, C., Biviano, A., & Perea, J. 1998, A&AS, 129, 399

Kent, S. M. 1985, ApJS, 59, 115

Knezek, P. M. 1993, Ph.D. Thesis, University of Massachusetts

Knezek, P. M. 1998, IAU Colloquium 171, ASP 170, The Low Surface Brightness Universe, 191

Kormendy, J. 1989, ApJ, 342, L63

Lauberts, A., & Valentijn, E. A. 1989, The Surface Photometry Catalogue of the ESO-Uppsala Galaxies, European Southern Observatory

Lewis, B. M. 1987, ApJS, 63, 515

Matthews, L. D., & Gallagher, J. S. 1997, AJ, 114, 1899

Matthews, L. D., & van Driel, W. 2000, A&AS, 143, 421

Matthews, L. D., van Driel, W., & Gallagher, J. S. 1998, AJ, 116, 1169

McGaugh, S. S., & Bothun, G. D. 1994, AJ, 107, 530

Melnick, J., & Quintana, H. 1981, AJ, 86, 1567

Nilson, P. 1973, Uppsala General Catalog of Galaxies, Uppsala Astron. Obs. Ann. Band 6

O'Neil, K., Bothun, G. D., & Cornell, M. 1997, AJ, 113, 1212

Pickering, T. E., Impey, C. D., van Gorkom, J. H., & Bothun, G. D. 1997, AJ, 114, 1858

Pickering, T. E., van Gorkom, J. H., Impey, C. D., & Quillen, A. C. 1999, AJ, 118, 765

Radford, S. J. E. 1992, A&A, 262, 13

Rhee, M.-H., & van Albada, T. S. 1996, A&AS, 115, 407

Roberts, M. S., & Haynes, M. P. 1994, ARAA, 32, 115

Sandage, A., & Tammann, G. A. 1981, A Revised Shapeley-Ames Catalog of Bright Galaxies, Carnegie Institution

Sanders, D. B., Solomon, P. M., & Scoville, N. Z. 1984, ApJ, 276, 182

Schmelz, J. T., Baan, W. A., Haschick, A. D., & Eder, J. 1986, AJ, 92, 1291

Schombert, J. 1998, AJ, 116, 1650

Schombert, J., Bothun, G. D., Schneider, S. E., & McGaugh, S. S. 1992, AJ, 103, 1107

Shostak, G. S. 1978, A&A, 68, 321

Sprayberry, D., Bernstein, G. M., Impey, C. D., & Bothun, G. D. 1995a, ApJ, 438, 72

Sprayberry, D., Impey, C. D., Bothun, G. D., & Irwin, M. J. 1995b, AJ, 109, 558

Sprayberry, D., Impey, C. D., Irwin, M. J., et al. 1993, ApJ, 417, 114

Staveley-Smith, L., & Davies, R. D. 1988, MNRAS, 231, 833

Thuan, T. X., Lipovetsky, V. A., Martin, J.-M., & Pustilnik, S. A. 2000, A&AS, 139, 1

Theureau, G., Bottinelli, L., Coudreau-Durand, N., et al. 1998, A&AS, 130, 333

Tifft, W. G., & Cocke, W. J. 1988, ApJS, 67, 1

van der Hulst, J. M., Skillman, E. D., Smith, T. R., Bothun, G. D., McGaugh, S. S., & de Blok, W. J. G. 1993, AJ, 106, 548

Verheijen, M. A. W. 1997, Ph.D. Thesis, University of Groningen

Walsh, W., Staveley-Smith, L., & Oosterloo, T. 1997, AJ, 113, 1591

Zwaan, M. A., van der Hulst, J. M., de Blok, W. J. G., & McGaugh, S. S. 1995, MNRAS, 273, L35